Histology and Synchrotron Radiation-Based Microtomography of the Inner Ear in a Molecularly Confirmed Case of CHARGE Syndrome

Rudolf Glueckert,[1,2] Helge Rask-Andersen,[4] Consolato Sergi,[5,6] Joachim Schmutzhard,[1] Bert Mueller,[7] Felix Beckmann,[8] Olaf Rittinger,[3,9] Lies H. Hoefsloot,[9] Anneliese Schrott-Fischer,[1]* and Andreas R. Janecke[10]

[1]Department of Otolaryngology, Medical University Innsbruck, Innsbruck, Austria

[2]University Hospital Innsbruck, Tiroler Landeskrankenanstalten Tilak, Austria

[3]Department of Paediatrics, Paracelsus Medical University Salzburg, Salzburg, Austria

[4]Department of Otolaryngology, University Hospital of Uppsala, Uppsala, Sweden

[5]Department of Pathology, Medical University Innsbruck, Innsbruck, Austria

[6]Department of Laboratory Medicine, University of Alberta, Edmonton, Canada

[7]University of Basel, Biomaterials Science Center, Basel, Switzerland

[8]GKSS-Research Centre, Institute for Materials Research, Geesthacht, Germany

[9]Department of Human Genetics, University Medical Centre Nijmegen, Nijmegen, the Netherlands

[10]Division of Clinical Genetics, Medical University Innsbruck, Innsbruck, Austria

CHARGE (Coloboma of the iris or retina, heart defects, atresia of the choanae, retardation of growth and/or development, genital anomalies, ear anomalies) syndrome (OMIM #214800) affects about 1 in 10,000 children and is most often caused by chromodomain helicase DNA-binding protein-7 (*CHD7*) mutations. Inner ear defects and vestibular abnormalities are particularly common. Specifically, semicircular canal (SCC) hypoplasia/aplasia and the presence of a Mondini malformation can be considered pathognomonic in the context of congenital malformations of the CHARGE syndrome. We obtained a temporal bone (TB) of a patient with CHARGE syndrome who died from bacteremia at 3 months of age. The clinical diagnosis was confirmed in the patient by direct DNA sequencing and the detection of a de novo, truncating *CHD7* mutation, c.6169dup (p.R2057fs). We assessed changes of the TB and the degree of neural preservation, which may influence the potential benefit of cochlear implantation. The TB was analyzed using synchrotron radiation-based micro computed tomography, and by light microscopy. The vestibular partition consisted of a rudimentary vestibule with agenesis of the SCCs. The cochlea was hypoplastic with poor or deficient interscaling and shortened (Mondini dysplasia). The organ of Corti had near normal structure and innervation. Modiolus and Rosenthal's canal were hypoplastic with perikarya displaced along the axon bundles into the internal acoustic meatus, which may be explained by the arrest or limited migration and translocation of the cell nuclei into the cochlear tube during development. © 2010 Wiley-Liss, Inc. © 2010 Wiley-Liss, Inc.

INTRODUCTION

CHARGE syndrome is a multiple malformation syndrome, originally defined by consensus diagnostic criteria, introduced by Blake et al. [1998]. Pagon et al. [1981] proposed the acronym CHARGE, describing the association of several anomalies: Coloboma of the iris or retina (C), heart defects (H), atresia of the choanae (A), retardation of growth and/or development (R), genital anomalies (G), ear anomalies (E). Abnormal semicircular canals (SCCs) and vestibular dysfunction are considered the most important and constant clinical characteristics for diagnosis [Abadie et al., 2000]. Additional malformations, in particular esophageal atresia and uni- or bilateral cleft/palate occur frequently. Surgical and intensive care are often required in the first year of life to treat congenital malformations and provide adequate nutritional intake, and most of these children survive and eventually participate in social life. Psychomotor development is generally delayed during the first years of life, and a typical behavioral pattern might be distinguished.

Abnormities have been found throughout the whole auditory system including pinnae, external auditory canal, middle ear, inner ear, and eustachian tube. External ear malformations are generally present in CHARGE syndrome and include lack of cartilage to cup-shaped ear with a hypoplastic lobule [Davenport et al., 1986]. Ear abnormalities have also been reported in the middle and inner ear [Wright et al., 1986; Blake et al., 1998; Tellier et al., 1998; Lalani et al., 2006]. Inner ear anomalies can be found in 90% of patients [Morgan et al., 1993; Abadie et al., 2000; Stromland et al., 2005]. Mondini dysplasia (CHARGE type) [Sekhar and Sachs, 1976] often occurs but is relatively unspecific to this syndrome since it is also observed in other deafness syndromes. However, labyrinthine dysplasia, such as cochlear hypoplasia and vestibular abnormalities are very common. Especially the absence/hypoplasia of one or all SCCs and hypoplastic incus are proposed to be the most specific anomalies of CHARGE-syndrome [Amiel et al., 2001; Verloes, 2005].

Hearing loss can therefore be both conductive and sensorineural, ranging from mild to severe. The inner ear histopathology of CHARGE from human autopsy studies has been reported in few cases, all before the molecular etiology of the disease had been established [Wright et al., 1986; Guyot et al., 1987; Schuknecht, 1993].

The disorder is caused by heterozygous loss-of-function mutations in the chromodomain helicase DNA-binding protein-7 (CHD7) gene. The gene product belongs to a large family of evolutionarily conserved proteins thought to play a role in chromatin organization. CHD7 is a regulatory element that potentially affects a large number of developmental pathways. This pleiotropic nature may explain the phenotypic spectrum seen in CHARGE patients. Here we present a morphological study in the first patient clinically and molecularly diagnosed with CHARGE syndrome.

CLINICAL REPORT

A diagnosis of CHARGE syndrome was made in a male born to healthy, unrelated parents because of bilateral cleft lip/palate,

coloboma on the choroid of both eyes, pulmonic stenosis and type II atrial septum defect, large abnormal ears with flattened helices, a square-shaped face, corpus callosum hypoplasia, malformation of the inner ear (see below), genital hypoplasia, and growth parameters at the 3rd centile. Autopsy and histology of cerebellum, basal ganglia, thalamus, thymus, thyroid gland, lung, gastrointestinal tract, kidney and adrenal gland, liver, pancreas, and spleen did not show any further abnormalities. The child had cyanosis, rapid deep breathing (80/min) and needed tracheal intubation. No hearing tests are available. The child died aged 3 months from bacteremia.

MATERIALS AND METHODS

Molecular Analysis

Informed consent for clinical molecular testing was obtained from the parents. All exons and flanking intronic sequences of CHD7 were PCR amplified and sequenced in both directions. PCR primers and conditions are available from the authors. The PCR fragment found to contain a heterozygous mutation in the patient was sequenced in both parents. Paternity was confirmed by genotyping a panel of microsatellite markers from different chromosomes.

Morphological Analyses

One temporal bone (TB) of a subject suspected for CHARGE syndrome was removed for morphologic, diagnostic reasons in the course of a routine autopsy. Ethical board approval for further research studies was obtained from the institutional board (study number EK1:06.10.06).

After opening the oval window for perilymphatic fixative penetration the TB was immersed in 4% paraformaldehyde (PFA) and 0.1% glutaraldehyde (GA) in 0.1 M phosphate-buffered saline (PBS), pH 7.4, for 14 days and postfixed in 1.5% OsO_4 for 60 min.

Three TBs from three different normal hearing individuals served as controls. Two inner ears were processed for synchrotron radiation-based micro computed tomography (SRμCT) and archival celloidin sections from another TB served to compare histology.

Synchrotron Radiation-Based Micro Computed Tomography

Three TBs were studied using SRμCT yielding combined information about the 3D gross morphology including visualization of the bony and membranous labyrinth structures. The inner ears were transferred to a plastic vial containing PBS and fixed at the high precision manipulator of the tomography set-up at the beamline W 2 (HASYLAB at DESY, Hamburg, Germany), operated by the GKSS-Research Center (Geesthacht, Germany) to acquire radiographic projections in the absorption contrast mode. Using photon energy of 35 keV, 6 tomograms each reconstructed from 1,441 projections with asymmetric rotation axis were obtained with a pixel size of 5.38 μm. The spatial resolution of the entire set-up determined by the modulation transfer function corresponded to 8.46 μm [Muller et al., 2002].

The data were binned before reconstruction by a factor of two to increase the density resolution. Tomograms were reconstructed slice-wise based on the filtered back-projection algorithm and combined to a single volumetric dataset as described previously [Fierz et al., 2008]. For 3D-visualisation the software VG Studio Max 1.2.1 (Volume Graphics, Heidelberg, Germany) was applied. The quantities such as the length of the cochlea were analyzed by means of dedicated software tools (IDL 7.0, ITT Visual Information Solutions, Boulder, CO) that allow manually selecting points on the trajectory to be extracted. This was performed along the most distal part of the osseous spiral lamina corresponding approximately to the level of the inner hair cells as described previously [Schmutzhard et al., 2009].

Histological Preparation

The CHARGE TB was decalcified with 10% EDTA solution for 4 weeks. The cochlea was separated from the vestibule and cut mid-modiolar. Specimens were dehydrated in ascending grades of alcohol and embedded in Spurr's low viscosity epoxy resin. Semithin sectioning was performed at a thickness of 2 μm with a Leica ® Ultracut S ultramicrotome and stained with Toluidine blue at 60°C. The control archival TB was decalcified with trichloric acid, embedded in celloidin and cut on a standard microtome in 25 μm thick sections that were consequently stained with haematoxilin–eosin.

RESULTS
Molecular Findings

Chromosome banding analysis was performed before a diagnosis of CHARGE syndrome was established in the patient, and showed a normal karyotype in peripheral leukocytes (46, XY; 500-band resolution). Sequencing of the coding region of the *CHD7* gene in DNA from leukocytes showed a heterozygous c.6169dupC (p.Arg2057fs) mutation in the patient, which was absent in samples from both parents. The mutation causes a premature stop codon after inclusion of two abnormal amino acids and predicts either severe truncation of the 2997-amino acid protein or nonsense-mediated RNA decay.

Morphology by Histology and SRμCT Analysis

SRμCT revealed that the cochlea consisted of only $1\frac{1}{2}$ turns and absent SCCs (Fig. 1A–C). The sensory epithelium was shortened to 20.9 mm in length (mean of three measurements, normal 31–37 mm) (Fig. 1A). Oval and round window appeared normal, and the otic capsule did not show any signs of atrophy or thickening. The ductus reunions was broad leading to a wide communication between cochlear duct and vestibule. The facial nerve had a regular course (Fig. 1B,C). The vestibular partition consisted of an underdeveloped vestibule with agenesis of SCCs. Only some rudiments from the ampullae's were present (Fig. 1B–D).

The vestibular aqueduct was around 1.2 mm in diameter (endolymphatic duct—ED, 0.8–1 mm in diameter) but lacked a distinct isthmus. It opened into the endolymphatic sac (ES) with characteristic foldings of the epithelium (Fig. 1E). The extraosseous part of the ES was not preserved as a whole in this specimen due to trimming of the TB (Fig. 1C–E) but comprised some typical tubular structure (not shown). The intraosseous part of the ES was a single lumen with few infoldings of the epithelium lining the sac (Fig. 1E). Both macula organs had normal size and showed a rich innervation by myelinated nerve fibers projecting into the vestibular nerve in the inner acousticus meatus (Fig. 2B,C). We were able to find a rudimentary crista structure (Fig. 2D) void of any myelinated nerve fibers only within the remnant of the lateral ampulla. Cochlear aqueduct, round window niche and round window membrane developed regularly (Fig. 2B,E). The inner acousticus meatus was a prominent structure in this shortened cochlea with diameters ranging from 5.5 to 5.7 mm at the level of cochlear and vestibular nerve anastomosis and 3.5–3.8 mm more proximal (Fig. 3A–C). Modiolus and Rosenthal's canal were hypoplastic with an osseous spiral lamina ending in a delicate hook like structure (Fig. 3B) and perikarya located along the axonal bundles into the internal acoustic meatus (IAM) (Fig. 3C). The lower basal turn appeared normal with an osseous spiral lamina densely packed with nerve fibers and plenty of spiral ganglion neurons. The middle ear was not preserved in this preparation.

To compare these morphological deviations with normal inner ear structure see Figure 4.

DISCUSSION

The results of this microanatomic study with molecular confirmation of the diagnosis and previous reports on morphology of the inner ear demonstrate the basis of the hearing loss in this syndrome. The vestibular and cochlear malformations argue for defective embryologic development. It has been reported that all the malformations in CHARGE syndrome occur early during the first trimester [Blake and Prasad, 2006]. There is a crucial stage of embryogenesis, when failure to rupture the primitive bucconasal membrane (35th to 38th day) brings about choanal atresia. Conotruncal cardiac defects can result from aberrations in cephalic neural crest cell migration during the 4th and 5th weeks after conception. The cochlear duct begins to develop around the 36th day, and the eyes develop between days 34 and 44 postconception, that is also the time during which many cranial nerves are developing [Blake and Prasad, 2006].

CHD7 is supposed to play an important role in early embryogenesis, and shows an ubiquitous expression in several fetal and adult tissues, such as neural epithelium, otic, and optic placodes, which are the primordial tissues giving rise to organs affected in CHARGE syndrome patients [Aramaki et al., 2007]. *CHD7* seems also to be widely expressed in fetal and adult tissues of humans, and is proposed to be a transcription regulator [Davenport et al., 1986]. The *CHD7* gene has been shown to be mutated in ∼2/3 of clinical CHARGE syndrome cases [Jongmans et al., 2006; Lalani et al., 2006]. Intronic mutations, exonic deletions missed by sequencing or UTR mutations may explain patients without detected mutations [Sanlaville and Verloes, 2007]. In addition, alterations of the semaphorin-3E gene have been reported in two patients with a CHARGE syndrome phenotype [Lalani et al., 2004]. The inner ear in this study showed a typical Mondini type dysplasia with hypoplastic modiolus, shortening of the cochlea and retardation of
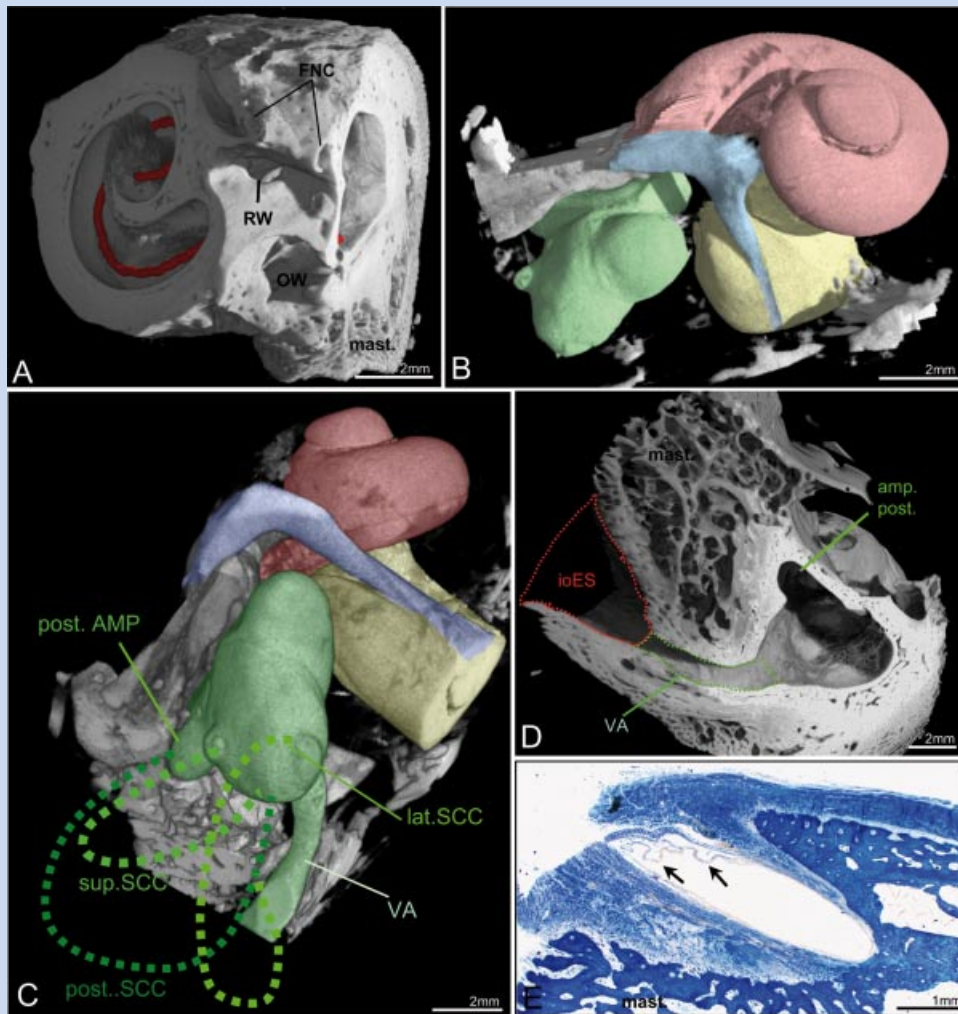
FIG. 1. A–D: 3D reconstructions from SRμCT data of the bone (A) and membranous labyrinth (B,C) in a patient suffered from CHARGE syndrome: Different anatomic regions are colored for clarity. E: histological section through the endolymphatic sac. A: demonstrates the normal oval- (OW) and round window (RW) and a shortened length of the sensory epithelium (red line). B,C: Exposes the 1.5 turns present in the cochlea (colored red). The vestibular region (colored green) consists of a vestibule with the cavities housing the utricle and saccule but no semicircular canals (SCC). The missing SCCs are delineated with green dotted lines. Only small remnants of the superior and lateral ampullae can be seen while the posterior ampulla is bigger. Internal acoustic meatus (yellow), facial nerve (blue). The vestibular aqueduct (VA-delineated with green lines) merges into the endolymphatic sac. The intraosseous part of the endolymphatic sac (ioES) is delineated with red lines. E: The ES in a histological section comprises the typical "wrinkled" epithelium (arrows). FNC-facial nerve canal, mast-mastoid, OC-organ of Corti, posterior (post.), superior (sup.), and lateral (lat.) SSC, post. AMP-, posterior ampulla. [Color figure can be viewed in the online issue, which is available at www.interscience.wiley.com.]

development of the vestibular system. The vestibular partition consisted of a rudimentary vestibule with agenesis of the SCCs which is a typical finding described before [Lemmerling et al., 1998; Morimoto et al., 2006]. In Jackler et al.'s [1987] work on congenital malformations of the inner ear the authors hypothesized that SCC aplasia was due to an arrest of embryogenesis in the 6th week of gestation. During that time the SCCs emerge from the vestibular appendage. An arrest of embryogenesis in the 7th week results in 1–1.5 turns or the Mondini type dysplasia [Jackler et al., 1987]. This arrest does not explain the middle ear malformations or other anomalies associated with CHARGE syndrome [Morimoto et al., 2006], but may explain for a variety of inner ear anomalies.

However, middle ear anomalies are not constant characteristics of this syndrome.

A vestibular aqueduct is considered enlarged if it is >1.5 mm in diameter and described as large ED and sac syndrome, LEDS [Valvassori and Clemis, 1978]. The ED was found to be present and not enlarged. We were not able to find signs of LEDS that are often associated with Mondini type malformations. Abadie et al. [2000] found normal vestibular aqueducts in 30 of 34 cases of CHARGE syndrome using CT scans. The intraosseous part of the ES showed only few infoldings and comprised a single volume without any tubular structure whereas the extraosseous part showed some tubules diverging from the main lumen. However, the extraosseous
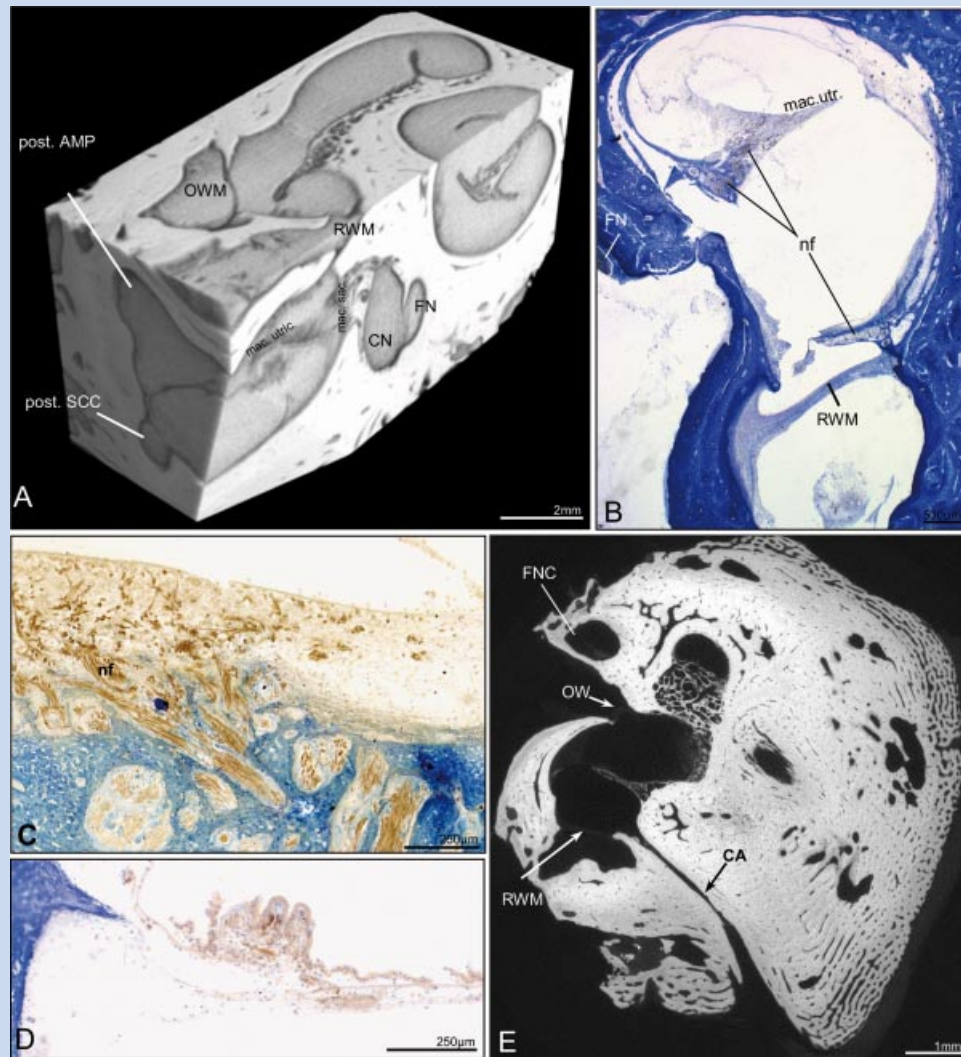
FIG. 2. SRμCT reconstructions and histological sections at the level of the round and oval windows and vestibular sensory epithelium: A: Synchrotron-based 3D reconstruction of inner ear membranous structures near oval (OW) and round window (RW). Macula organs can be identified by higher absorption in SRμCT imaging. The histological section in (B) shows nerve fibers (nf) diverging to the macula utriculi and a normal round window membrane (RWM). C: A rich nerve fiber (nf) network near the macula sacculi and in (D) a rudimentary crista structure void of any myelinated nerve fibers in the posterior ampulla. The cochlear aqueduct (CA) in (E) shows normal anatomy. Posterior ampulla, post. AMP; macula utriculi, mac. utric.; macula sacculi, mac. sac.; facial nerve, FN.; cochlear nerve, CN; posterior semicircular canal, post. SCC; oval window, OW; round window, RW; facial nerve canal, FNC. [Color figure can be viewed in the online issue, which is available at www.interscience.wiley.com.]

part of the sac was only partly preserved in our preparation. This primitive-appearing, pouch-like, single-lumen ES can be present as late as 2 weeks after gestation as described by Ng and Linthicum [1998]. The transition from simple saccular structure to a tubular system in humans is characteristic of the ES morphologic maturation process. At the age of 2–3 year the ES appears as a complex network of interconnected tubules known from the mature adult inner ear [Kodama and Sando, 1982]. Hence, length and differentiation of the ED/ES system was normal.

Both the saccule and utricular neuroepithelium was present with distribution of sensory epithelial cells and an otoconial membrane. The epithelium was also supplied with nerve fibers suggesting that the otolithic organs were fairly well intact although no clinical data

are available to prove. Vestibular dysfunction was reported to be a constant clinical sign in CHARGE syndrome and has very good sensitivity for confirming the diagnosis [Abadie et al., 2000]. The most frequent anomaly in their study (17 CHARGE patients) was bilateral complete absence of the three SCCs always associated with vestibular dysfunction. Otolith function varies from normal to no responses and is important for rehabilitation strategies as vertical and horizontal movements of translation can be used to help the child organize its balance [Abadie et al., 2000]. The ampullae in the case presented here showed abnormal structure suggesting impaired function. No normal cristae were observed and the SCCs were lacking with only a short stump preserved.
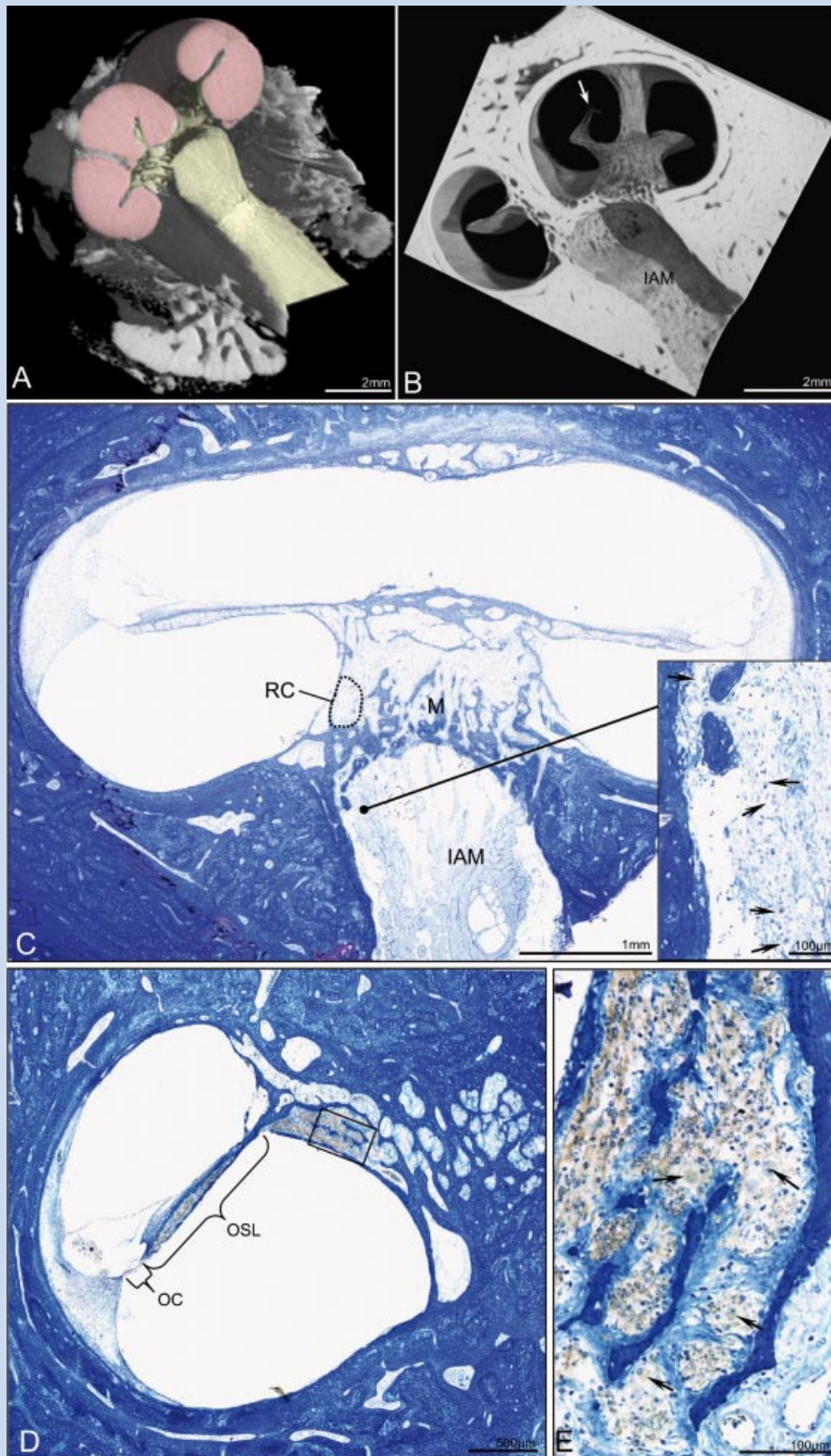
FIG. 3. SRμCT and histology of the basal and middle turn of the cochlea and the internal acoustic meatus. A: Some structures are highlighted in yellow (content of the modiolus, osseous spiral lamina, and inner acousticus meatus) and red (peri- and endolymphatic compartments). B: A central column connects the hypoplastic modiolus with the otic capsule, the inner an acousticus meatus (IAM). The delicate osseous spiral lamina ends in a hook-like structure (arrow). Histological sections of the middle (C) and basal turn (D,E) of the cochlea in the CHARGE TB. C: The modiolus (M) and the Rosenthal's canal (RC-delineated here with a dotted line) contains several neural perikarya but neuron cell bodies are also located in the internal acoustic meatus (IAM) (inset showing a magnified view—arrows pointing to perikarya of the spiral ganglion neurons). D: The basal turn appears normal with an intact organ of Corti (OC) and a spiral lamina (OSL) containing numerous axons (D). Framed area is seen with light microscopy in (E) Rosenthal's canal contains several neural perikarya (arrows). [Color figure can be viewed in the online issue, which is available at www.interscience.wiley.com.]
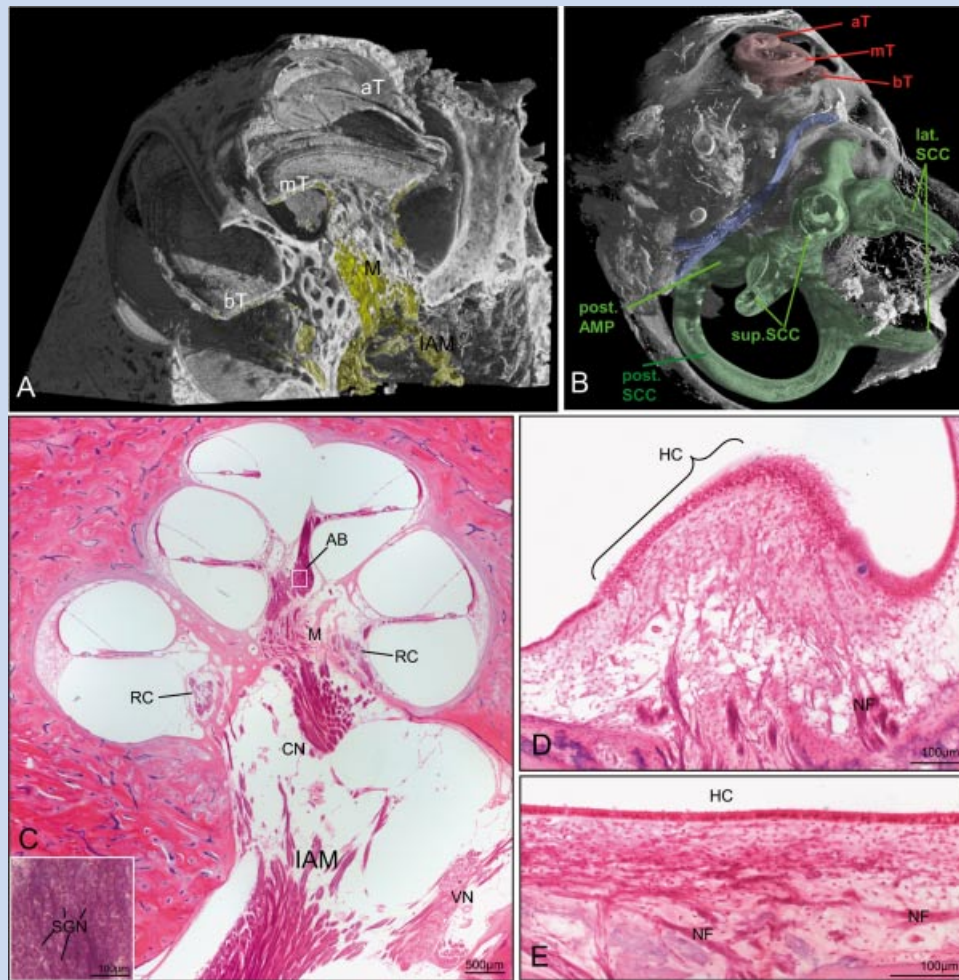
FIG. 4. SRμCT and histology of normal control temporal bones. A: Displays the 3D SRμCT view of the bony and membranous portion of a normal cochlea with 2.5 turns (bT, basal turn; mT, middle turn; aT, apical turn) and a regularly developed modiolus (M). The cochlear nerve is segmented and colored yellow. Inner acousticus meatus, IAM. B: 3D reconstruction of SRμCT data from another temporal bone illustrating the fluid spaces and membranous part of the vestibular labyrinth (colored green), the facial nerve (blue) and the cochlea (red). The semicircular canals (SCCs) are partly cut in this view. Posterior (post.), superior (sup.), and lateral (lat.) SSC, post. AMP, posterior ampulla; bT, basal turn; mT, middle turn; aT, apical turn of the cochlea. C–E: A celloidin embedded and sectioned human temporal bone exhibits normal morphology. C: Midmodiolar section displays a well-developed modiolus (M) with spiral ganglion neurons (SGNs) magnified in the inset. Neurons are only located in Rosenthal's canal (RC) and the apical bulge (AB). The central processes of SGNs coalesce to the cochlear nerve (CN) that unites with the vestibular nerve (VN) in the bony inner acoustic meatus (IAM). D: Regularly developed crista ampullaris, the sensory receptor apparatus that responds to angular acceleration (rotational motion). Sensory hair cells (HC) are located as a single layer on the surface of the ridge of tissue, NF-nerve fibres. E: The macula sacculi transmits linear acceleration (linear motion and gravity) to the central nervous system. HC, hair cells; NF, nerve fibers. [Color figure can be viewed in the online issue, which is available at www.interscience.wiley.com.]

The cochlea was hypoplastic with a modiolus of the Mondini type. Interestingly neural perikarya were found both in the RC but also displaced along the axon bundles into the IAM. Thus, the number and preservation of neural perikarya was considerable in our specimen. Tomura et al. [1995] pointed out that the size and shape of the IAM is known to be variable. The IAM proved to be too variable in its morphology and course to allow consistent measurements by computer tomography [Purcell et al., 2003]. The retention of perikarya within the meatus may be explained by the arrest or limited migration and translocation of the cell nuclei into the cochlea along the tube during development and is also described in congenital disorders such as Turner syndrome [Fish et al., 2009], Pendred syndrome [Yang et al., 2005], trisomy 13 [Tomoda et al., 1983], and trisomy 22 [Ohtani et al., 2001]. Neural structures may partly be dislodged into the malformed internal meatus. Mondini type dysplasia is frequently described in CHARGE patients but it is not a constant feature.

There are only few reports on histology or high-resolution tomography on the hearing organ in CHARGE patients. Wright et al. [1986] acquired the TBs of two infants who died soon after birth. Hearing test was also not available. The principal findings consisted of normal external auditory canals, dysplastic ossicles,

absence of oval and round windows, normal cochleae in one case and short cochleae (20.9 mm) in the other and varying degrees of hypoplasia of the vestibular sense organs and nerves. Guyot et al. [1987] reported the TB findings of a 7-month-old female infant with CHARGE association that showed Mondini dysplasia of the pars inferior (cochlea and saccule) and absence of the pars superior (vestibule and utricle). Schuknecht [1993] described two cases of CHARGE. In one case, the external auditory canals, tympanic membranes, mallei and incudes were normal; there was a severe dysplasia of the stapes, oval windows were missing. The other case presented a single turn cochlea on the right and one-half turn on the left. In both ears, a few cochlear neurons were present in the hypoplastic modiolus. Maculae sacculi were present but hypoplastic and the utricles and SCCs were absent.

Computed tomography (CT) applied in the daily routine has reached a spatial resolution below 1 mm; however, this resolution is not fine enough to detect slight aberrations of the human inner ear. Here, synchrotron radiation sources provide the necessary flux to generate monochromatic X-rays of enough intensity to perform CT measurements within reasonable periods of time. The main advantage with respect to conventional μCT is the much higher photon flux, which offers to eliminate all photons but the ones of selected energy, and still maintain a reasonable period of time for data acquisition. These high-resolution CT investigations cannot be performed in vivo, since the high doses create nontolerable damages. TB CT and magnetic resonance imaging (MRI) studies of CHARGE patients have shown characteristic abnormalities including hypoplastic incus, decreased number of cochlear turns (Mondini defect), and in particular absent SCCs [Amiel et al., 2001]. Morimoto et al. [2006], studied 13 CHARGE patients. They found that 20 of 26 (77%) ears demonstrated cochlear aperture atresia. Four of these ears were evaluated with MRI and were found to lack a cochlear nerve. Twenty-one of 26 (81%) cochleae had some form of dysplasia. All cases demonstrated absent SCCs. Twenty-three of 26 (93%) ossicles were dysplastic with ankylosis.

Variations in the TB anatomy associated with CHARGE may lead to increased technical challenges and risk to the facial nerve during CI. Individual outcomes and obtained benefit after implantation may vary [Bauer et al., 2002]. Parents should be counseled thoroughly and have appropriate expectations before proceeding with implantation. According to Lanson et al. [2007] CI in children with sensorineural hearing loss and CHARGE syndrome can lead to varying, but limited degrees, of auditory benefit with no increase in surgical complications. Although the implant enhanced the children's "connectivity" to the environment, it did not promote the development of oral language skills in this population.

The TB anatomy of the presented case points out the presence of neuronal structures in a malformed inner ear. Displaced but preserved neural perikarya may also explain the benefits of CI in patients with more advanced cochlear deformations as long as a cochlear neural structure is confirmed with MRI. For the developmental outcome of children with CHARGE syndrome [Blake et al., 1998; Searle et al., 2005] of particular importance is the early diagnosis of hearing and visual loss so that use of appropriate auditory and visual aids can be initiated as soon as possible, allowing for optimal language and communication development. Furthermore, detailed published information beyond early childhood are lacking in CHARGE syndrome and it is only within the last 20 years that advances in intensive care have allowed children with CHARGE syndrome to survive into adolescence and adulthood. For this reason the timely treatment of hearing loss as well as visual impairment is fundamental.

REFERENCES

Abadie V, Wiener-Vacher S, Morisseau-Durand MP, Poree C, Amiel J, Amanou L, Peigne C, Lyonnet S, Manac'h Y. 2000. Vestibular anomalies in CHARGE syndrome: Investigations on and consequences for postural development. Eur J Pediatr 159:569–574.

Amiel J, ttiee-Bitach T, Marianowski R, Cormier-Daire V, Abadie V, Bonnet D, Gonzales M, Chemouny S, Brunelle F, Munnich A, Manach Y, Lyonnet S. 2001. Temporal bone anomaly proposed as a major criteria for diagnosis of CHARGE syndrome. Am J Med Genet 99:124–127.

Aramaki M, Kimura T, Udaka T, Kosaki R, Mitsuhashi T, Okada Y, Takahashi T, Kosaki K. 2007. Embryonic expression profile of chicken CHD7, the ortholog of the causative gene for CHARGE syndrome. Birth Defects Res A Clin Mol Teratol 79:50–57.

Bauer PW, Wippold FJ, Goldin J, Lusk RP. 2002. Cochlear implantation in children with CHARGE association. Arch Otolaryngol Head Neck Surg 128:1013–1017.

Blake KD, Prasad C. 2006. CHARGE syndrome. Orphanet J Rare Dis 1:34.

Blake KD, Davenport SL, Hall BD, Hefner MA, Pagon RA, Williams MS, Lin AE, Graham JM Jr. 1998. CHARGE association: An update and review for the primary pediatrician. Clin Pediatr (Phila) 37:159–173.

Davenport SL, Hefner MA, Mitchell JA. 1986. The spectrum of clinical features in CHARGE syndrome. Clin Genet 29:298–310.

Fierz FC, Beckmann F, Huser M, Irsen SH, Leukers B, Witte F, Degistirici O, Andronache A, Thie M, Muller B. 2008. The morphology of anisotropic 3D-printed hydroxyapatite scaffolds. Biomaterials 29: 3799–3806.

Fish JH III, Schwentner I, Schmutzhard J, Abraham I, Ciorba A, Martini A, Sergi C, Schrott-Fischer A, Glueckert R. 2009. Morphology studies of the human fetal cochlea in turner syndrome. Ear Hear 30:143–146.

Guyot JP, Gacek RR, DiRaddo P. 1987. The temporal bone anomaly in CHARGE association. Arch Otolaryngol Head Neck Surg 113:321–324.

Jackler RK, Luxford WM, House WF. 1987. Congenital malformations of the inner ear: A classification based on embryogenesis. Laryngoscope 97:2–14.

Jongmans MC, Admiraal RJ, van der Donk KP, Vissers LE, Baas AF, Kapusta L, van Hagen JM, Donnai D, de Ravel TJ, Veltman JA, Geurts van KA, De Vries BB, Brunner HG, Hoefsloot LH, van Ravenswaaij CM. 2006. CHARGE syndrome: The phenotypic spectrum of mutations in the CHD7 gene. J Med Genet 43:306–314.

Kodama A, Sando I. 1982. Postnatal development of the vestibular aqueduct and endolymphatic sac. Ann Otol Rhinol Laryngol 96:3–12.

Lalani SR, Safiullah AM, Molinari LM, Fernbach SD, Martin DM, Belmont JW. 2004. SEMA3E mutation in a patient with CHARGE syndrome. J Med Genet 41:e94.

Lalani SR, Safiullah AM, Fernbach SD, Harutyunyan KG, Thaller C, Peterson LE, McPherson JD, Gibbs RA, White LD, Hefner M, Davenport SL, Graham JM, Bacino CA, Glass NL, Towbin JA, Craigen WJ, Neish SR, Lin AE, Belmont JW. 2006. Spectrum of CHD7 mutations in 110 individuals with CHARGE syndrome and genotype-phenotype correlation. Am J Hum Genet 78:303–314.

Lanson BG, Green JE, Roland JT Jr, Lalwani AK, Waltzman SB. 2007. Cochlear implantation in Children with CHARGE syndrome: Therapeutic decisions and outcomes. Laryngoscope 117:1260–1266.

Lemmerling M, Dhooge I, Mollet P, Mortier G, Van CP, Kunnen M. 1998. CT of the temporal bone in the CHARGE association. Neuroradiology 40:462–465.

Morgan D, Bailey M, Phelps P, Bellman S, Grace A, Wyse R. 1993. Ear-nose-throat abnormalities in the CHARGE association. Arch Otolaryngol Head Neck Surg 19:49–54.

Morimoto AK, Wiggins RH, Hudgins PA, Hedlund GL, Hamilton B, Mukherji SK, Telian SA, Harnsberger HR. 2006. Absent semicircular canals in CHARGE syndrome: Radiologic spectrum of findings. Am J Neuroradiol 27:1663–1671.

Muller B, Beckmann F, Huser M, Maspero F, Szekely G, Ruffieux K, Thurner P, Wintermantel E. 2002. Non-destructive three-dimensional evaluation of a polymer sponge by micro-tomography using synchrotron radiation. Biomol Eng 19:73–78.

Ng M, Linthicum FH. 1998. Morphology of the developing human endolymphatic sac. Laryngoscope 108:190–194.

Ohtani I, Kano M, Sagawa Y, Ogawa H, Suzuki C. 2001. Temporal bone histopathology in trisomy 22. Int J Pediatr Otorhinolaryngol 59:137–141.

Pagon RA, Graham JM Jr, Zonana J, Yong SL. 1981. Coloboma, congenital heart disease, and choanal atresia with multiple anomalies: CHARGE association. J Pediatr 99:223–227.

Purcell D, Johnson J, Fischbein N, Lalwani AK. 2003. Establishment of normative cochlear and vestibular measurements to aid in the diagnosis of inner ear malformations. Otolaryngol Head Neck Surg 128:78–87.

Sanlaville D, Verloes A. 2007. CHARGE syndrome: An update. Eur J Hum Genet 15:389–399.

Schmutzhard J, Schwentner I, Glueckert R, Sergi C, Beckmann F, Abraham I, Riechelmann H, Schrott-Fischer A, Muller B. 2009. Pelizaeus Merzbacher disease: Morphological analysis of the vestibulo-cochlear system. Acta Otolaryngol 129:1395–1399.

Schuknecht HF. 1993. Developmental defects. In: Febiger C, Lea HC. editors. Pathology of the ear. Philadelphia: pp. 115–189.

Searle LC, Graham JM Jr, Prasad C, Blake KD. 2005. CHARGE syndrome from birth to adulthood: An individual reported on from 0 to 33 years. Am J Med Genet Part A 133A:344–349.

Sekhar HK, Sachs M. 1976. Mondini defect in association with multiple congenital anomalies. Laryngoscope 86:117–125.

Stromland K, Sjogreen L, Johansson M, Ekman Joelsson BM, Miller M, Danielsson S, Billstedt E, Gillberg C, Jacobsson C, Norinder JA, Granstrom G. 2005. CHARGE association in Sweden: Malformations and functional deficits. Am J Med Genet Part A 133A:331–339.

Tellier AL, Cormier-Daire V, Abadie V, Amiel J, Sigaudy S, Bonnet D, Lonlay-Debeney P, Morrisseau-Durand MP, Hubert P, Michel JL, Jan D, Dollfus H, Baumann C, Labrune P, Lacombe D, Philip N, LeMerrer M, Briard ML, Munnich A, Lyonnet S. 1998. CHARGE syndrome: Report of 47 cases and review. Am J Med Genet 76:402–409.

Tomoda K, Shea JJ, Shenefelt RE, Wilroy RS. 1983. Temporal bone findings in trisomy 13 with cyclopia. Arch Otolaryngol 109:553–558.

Tomura N, Sashi R, Kobayashi M, Hirano H, Hashimoto M, Watarai J. 1995. Normal variations of the temporal bone on high-resolution CT: Their incidence and clinical significance. Clin Radiol 50:144–148.

Valvassori GE, Clemis JD. 1978. The large vestibular aqueduct syndrome. Laryngoscope 88:723–728.

Verloes A. 2005. Updated diagnostic criteria for CHARGE syndrome: A proposal. Am J Med Genet Part A 133A:306–308.

Wright CG, Brown OE, Meyerhoff WL, Rutledge JC. 1986. Auditory and temporal bone abnormalities in charge association. Ann Otol Rhinol Laryngol 95:480–486.

Yang JJ, Tsai CC, Hsu HM, Shiao JY, Su CC, Li SY. 2005. Hearing loss associated with enlarged vestibular aqueduct and Mondini dysplasia is caused by splice-site mutation in the PDS gene. Hear Res 199:22–30.